Neutron-proton effective range parameters and zero-energy shape dependence

R. W. Hackenburg*
Physics Department, Brookhaven National Laboratory, Upton, New York 11973, USA
(Received 22 March 2005; revised manuscript received 30 January 2006; published 7 April 2006)

The low-energy *np* elastic-scattering parameters, including the zero-energy free-proton cross section σ_0, are determined with a substantially improved precision over previous values, using available *np*-scattering data below 3 MeV. The method includes a careful handling of a correlation between the singlet and triplet effective ranges which does not seem to have been previously treated. This correlation is responsible for a large systematic error in the singlet effective range and spoils a model-independent determination of the zero-energy triplet effective range. It is shown that improved cross section measurements between 20 and 600 keV (laboratory neutron energy) are needed to overcome the degrading effect of this correlation. The values obtained for the zero-energy cross section and the scattering lengths and effective ranges for the singlet and triplet are: $\sigma_0 = 20.4278(78)$ b, $a_t = 5.4112(15)$ fm, $a_s = -23.7148(43)$ fm, $r_t = 1.7436(19)$ fm, $r_s = 2.750(18)$ fm (systematic error: -0.059 fm). The widely used measurement of the zero-energy free-proton elastic cross section from W. Dilg, Phys. Rev. C **11**, 103 (1975), appears to be in error.

DOI: 10.1103/PhysRevC.73.044002 PACS number(s): 13.75.Cs, 25.40.Dn, 28.20.Cz, 29.85.+c

This article presents a model-independent method for determining the zero-energy cross section σ_0 and effective-range theory (ERT) parameters for *np* elastic scattering from low-energy data. The method is similar to that presented in Ref. [1] but contains some improvements that permit the zero-energy triplet effective range to be obtained from data. It is demonstrated that there is a range of energy most sensitive to a determination of this quantity and that better measurements are needed in that range, if it is to be obtained with sufficient precision to be of any use in comparing predictions from *NN* potential models.

NN potential models [2–5] can determine the ERT parameters, but small errors are introduced if low-energy data are not included (or are inaccurate) in the partial-wave analyses used to fit the model parameters [3]. Because *NN* potential models are often used in low-energy applications [6–8], it is important that they incorporate accurate low-energy data. Some *NN* potential models [5,9,10] use the Dilg measurement of σ_0, some models [2–4,8,11,12] use an average of the Dilg and Houk values, but none seem to use the more precise Koester *et al*. value (Table I).

The Dilg determination of σ_0 is the only one that required molecular corrections but did not obtain them as part of the experiment. That experiment performed measurements on water and three hydrocarbons at a single energy, 132 eV, where the molecular corrections are small but not negligible. There was, therefore, no way of determining the molecular corrections, which require measurements at two or more energies for each target. The corrections used were asymptotic extrapolations to 132 eV from values taken from the literature, which described scattering on water and benzene at energies from about 1 to 15 eV. Prior to the Koester *et al*. σ_0, the Dilg σ_0 was not quite significantly deviant from the others, taken individually, because of their large errors. With the Koester *et al*. σ_0, and the result from this work, this is no longer true. All other determinations of σ_0, whether requiring molecular corrections or not, are in good agreement with each other and substantially deviant from the Dilg σ_0.

ERT gives the exact neutron-proton *s*-wave elastic cross section as [18,19]

$$\sigma = \tfrac{3}{4}\sigma_t + \tfrac{1}{4}\sigma_s, \tag{1}$$

$$\sigma_d = 4\pi \Big/ \left\{\left[a_d^{-1} - \tfrac{1}{2}\rho_d(0,T)p^2\right]^2 + p^2\right\}, \tag{2}$$

where the subscript d is t for the triplet or s for the singlet, a_d is the scattering length, and $\rho_d(0,T)$ is the energy-dependent effective range. T and p are the center-of-mass (c.m.) kinetic energy and momentum ($\hbar = c = 1$), with

$$\begin{aligned} E &= m_n + m_p + T = \sqrt{p^2 + {m_n}^2} + \sqrt{p^2 + {m_p}^2}, \\ p^2 &= \tfrac{1}{4}\left[E^2 - 2\left(m_n^2 + m_p^2\right) + \left(m_n^2 - m_p^2\right)^2 / E^2\right], \end{aligned} \tag{3}$$

where E is the total, relativistic energy in the c.m. The partial cross section has a pole at $p = i\gamma_d$, where γ_d is the scattering wave number, given by $\gamma_d^2 = -p^2$ from Eq. (3) for $T = -\epsilon_d$, or $E = m_n + m_p - \epsilon_d$, where ϵ_d is the binding energy. In terms of the asymptotic (free particle) *np* wave function $v_d(T)$ and the exact (interacting) *np* wave function $u_d(T)$, both of which implicitly depend on the neutron-proton separation r, the function $\rho_d(T_a, T_b)$ is defined as [20]

$$\rho_d(T_a, T_b) \equiv 2\int_0^\infty dr\, [v_d(T_a)v_d(T_b) - u_d(T_a)u_d(T_b)]\,,$$

where ρ_d, v_d, u_d are ρ_t, v_t, u_t for the triplet and ρ_s, v_s, u_s for the singlet and where T_a and T_b are any two values of the c.m. kinetic energy. This definition satisfies Eq. (2) exactly for $T_a = 0$ and $T_b = T$. The wave function u_d, but not v_d, depends on the shape of the nuclear potential, and this shape dependence manifests itself as energy dependence of ρ_d.

As long as p^{-1} is much larger than the well size, the detailed shape of the nuclear potential can have only a small effect on the spectrum. The shape-independent approximation replaces

*Electronic address: hack@bnl.gov

 ©2006 The American Physical Society

TABLE I. The σ_0 data considered for the fits. The χ^2 are calculated with respect to the result from this work.

Reference	Year	σ_0(b)	χ^2	Included in fits?
[13] Melkonian	1949	20.360(50)	1.84	Yes[a]
[14] Houk	1971	20.436(23)	0.13	Yes
[15] Dilg	1975	20.491(14)	20.4	No
[16] Koester *et al.*,	1990	20.420(10)	0.60	No[b]

[a]Error shown as adjusted by Ref. [17].
[b]Derived from data included in Table III.

$\rho_d(0, T)$ with the constant r_d,

$$\sigma_d \cong 4\pi \Big/ \left[\left(a_d^{-1} - \tfrac{1}{2} r_d p^2\right)^2 + p^2\right]. \quad (4)$$

For the triplet only, r_t is taken as $r_t = \rho_t(0, -\epsilon_t)$, the "mixed effective range," given exactly as [20]

$$\rho_d(0, -\epsilon_d) = 2\gamma_d^{-1}\left(1 - 1/a_d\gamma_d\right). \quad (5)$$

A measured elastic cross section σ_p at p may be used to determine r_s as r_{sp}, the apparent singlet effective range at p, through (1), (4), and the parameters a_t, a_s, and r_t, thus

$$r_s = 2p^{-2}\left(a_s^{-1} + \sqrt{4\pi/\sigma_{sp} - p^2}\right),$$

where $\sigma_{sp} \equiv 4\sigma_p - 3\sigma_t(p)$ is the estimated singlet partial cross section and $\sigma_t(p)$ is the theoretical triplet partial cross section, obtained with Eq. (4).

In principle, $\rho_d(0, 0) = \lim_{T\to 0} \rho_d(0, T)$ approximates $\rho_d(0, T)$ better than $\rho_d(0, -\epsilon_d)$ does, where the limit expresses the experimental condition that the variation with decreasing energy becomes smaller than the statistical error. Define Δr_d such that $\rho_d(0, 0) = \rho_d(0, -\epsilon_d) + \Delta r_d$. The condition $\Delta r_d \neq 0$ is referred to here as "zero-energy shape dependence." The (zero-energy) apparent singlet effective range $r_{s0} \equiv \lim_{T\to 0} r_{sp}$ is an approximation to $\rho_s(0, 0)$ with a systematic error $(\delta r_s)_{\Delta r_t}$, thus,

$$\begin{aligned} &\rho_s(0, 0) = r_{s0} + (\delta r_s)_{\Delta r_t}, \\ &(\delta r_s)_{\Delta r_t} \equiv \int_{r_t}^{r_t + \Delta r_t} dr_t \, (\partial r_s/\partial r_t) = \langle \partial r_s/\partial r_t \rangle \, \Delta r_t, \quad (6) \\ &\partial r_s/\partial r_t = -3\sigma_t^2\left(a_t^{-1} - \tfrac{1}{2} r_t p^2\right) \Big/ \sigma_s^2\left(a_s^{-1} - \tfrac{1}{2} r_s p^2\right). \end{aligned}$$

The measurements and their uncertainties are:

$\sigma_0 \pm \delta\sigma_0$ the zero-energy elastic cross section
$a_c \pm \delta a_c$ the parahydrogen coherent scattering length
$\sigma_p \pm \delta\sigma_p$ the elastic cross section at c.m. momentum p.

The uncertainties $\delta\sigma_0$, δa_c, and $\delta\sigma_p$ are small and independent. Because its uncertainty is utterly negligible compared to the others, ϵ_t is taken as exact. The zero-energy (free proton) elastic cross section is given by Eq. (1), taking $p = 0$ in (2), thus

$$\sigma_0 = \pi\left(3a_t^2 + a_s^2\right). \quad (7)$$

The parahydrogen coherent scattering length is [21]

$$a_c \equiv \tfrac{2}{3} a_t + \tfrac{1}{2} a_s. \quad (8)$$

TABLE II. The a_c data considered for the fits.

Reference	Year	a_c (fm)	χ^2	Included in fits?
[14] Houk	1971	−3.7210(40)	23.9	No
[22] Koester	1971	−3.7400(30)	0.04	Yes
[23] Callerame	1975	−3.7330(40)	14.3	No
[24] Koester and Nistler	1975	−3.7406(11)	0	Yes[a]

[a]Value shown as adjusted by Ref. [25].

The measurements of σ_0, a_c, and σ_p used in the fits are shown in Tables I, II, and III. The χ^2 are calculated from the parameters from this work. The value used for ϵ_t is the deuteron binding energy from [45], $\epsilon_t = 2.224\,566\,14(41)$ MeV. The physical constants used are from [46]. Because a_t and a_s are correlated, σ_0, a_c, and r_{s0} are taken as the fit variables, with

$$\begin{aligned} s &\equiv \sqrt{\tfrac{1}{12}\left(\sigma_0/\pi - a_c^2\right)}, \\ a_s &= \tfrac{1}{2} a_c - 3s, \quad a_t = \tfrac{1}{2} a_c + s. \end{aligned}$$

Contributions from higher waves increase the cross section and decrease the apparent singlet effective range if not accounted for. Rather than explicitly account for higher waves, a series of maximum-energy truncations are made, and a fit done to each of the truncated data sets. Table IV shows the fit results. The fit parameter σ_0 is determined almost entirely by the lowest-energy data, and the fit parameter a_c almost entirely by the a_c data, so these are very nearly independent of $T_{\max}$. The decline of r_{s0} and the increase in χ^2_ν with $T_{\max}$ above

TABLE III. The *np* total cross-section data used in the fits, from CINDA [26] and the literature. The data are truncated at 15 MeV.

Ref.	First Author	N	Average unc. (perc.)	Average χ^2	Min. energy (MeV)	Max. energy (MeV)
[16]	Koester	1	0.15	1.53	0.002	0.002
[27]	Kirilyuk	2	0.14	0.44	0.002	0.145
[28]	Fujita	1	0.13	0.13	0.024	0.024
[29]	Allen	5	2.60	0.26	0.06	0.55
[30]	Bailey	15	3.80	0.97	0.35	6.0
[17][a]	Engelke	2	0.25	2.70	0.493	3.186
[31][a]	Poenitz	3	0.30	2.37	0.509	2.003
[32]	Lampi	6	2.20	0.62	0.798	4.97
[33][a]	Fields	2	0.39	0.65	1.005	2.53
[34]	Koester	2	1.60	0.96	1.3	2.1
[35][a]	Storrs	1	0.54	0.04	1.312	1.312
[36]	Schwartz	1652	1.50	0.85	1.447	14.97
[37]	Davis	21	0.94	1.47	1.5	14.995
[38][b]	Clement	158	0.98	1.12	2.0	14.938
[39]	Nereson	38	10.00	0.07	2.95	13.1
[40][a]	Hafner	1	0.38	0.18	4.748	4.748
[41][b]	Larson	218	1.60	0.96	5.0	14.9
[42][b]	Foster	111	2.10	1.17	5.0	14.7
[43]	Cook	2	1.70	0.97	14.1	15.0

[a]Energy as adjusted by Ref. [44].
[b]These data are truncated below the minimum energy shown.

TABLE IV. The shape-independent fits. The fit parameters are σ_0, a_c, and r_{s0}. $T_{\max}$ is the maximum neutron kinetic energy in the lab and $\chi^2_\nu \equiv \chi^2/\nu$, with ν the degrees of freedom.

$T_{\max}$(MeV)	σ_0 (b)	a_c (fm)	r_{s0} (fm)	a_t (fm)	a_s (fm)	$\rho_t(0,-\epsilon_t)$ (fm)	χ^2_ν	ν
15	20.4109(61)	−3.74096(96)	2.7567(98)	5.4079(12)	−23.7057(34)	1.7394(16)	0.881	2242
10	20.4270(61)	−3.74064(96)	2.793(10)	5.4110(12)	−23.7144(34)	1.7434(16)	0.840	1944
5	20.4347(68)	−3.74049(98)	2.810(14)	5.4125(14)	−23.7186(38)	1.7452(17)	0.794	1258
4	20.4302(72)	−3.74055(98)	2.780(15)	5.4117(14)	−23.7161(40)	1.7442(18)	0.780	1077
3[a]	**20.4278(78)**	**−3.7406(10)**	**2.750(18)**	**5.4112(15)**	**−23.7148(43)**	**1.7436(19)**	**0.749**	**817**
2	20.4276(99)	−3.7406(10)	2.745(30)	5.4112(19)	−23.7147(54)	1.7436(24)	0.660	389
1	20.427(11)	−3.7405(10)	2.695(55)	5.4110(21)	−23.7142(62)	1.7434(27)	1.092	18

[a]This fit, shown in bold, is chosen as the best.

5 MeV may reasonably be interpreted as being caused by contributions from higher waves. Below 5 MeV, the variations in fit values of r_{s0} are not quite significant and are in the wrong direction for them to be the result of higher waves. Based on the phase shifts of *np* partial waves from Table V of Ref. [2], the net contribution from higher waves is much less than half the size of the statistical errors for the $T_{\max} = 3$ MeV data. Systematic errors introduced by ignoring higher waves are therefore negligible for the fits with $T_{\max} \leqslant 3$ MeV. Systematic errors introduced by ignoring the energy dependence of the effective ranges are similarly insignificant. The $T_{\max} = 3$ MeV fit is taken as the best fit; it has nearly the lowest χ^2_ν, while also having nearly the smallest errors for the fit parameters. The shape-independent parameters are determined to be

$$\begin{aligned} \sigma_0 &= 20.4278 \pm 0.0078\text{b}, \\ a_c &= -3.7406 \pm 0.0010\,\text{fm}, \\ r_{s0} &= 2.750 \pm 0.018_{\text{stat}} - 0.059_{\text{syst}}\,\text{fm}, \\ a_t &= 5.4112 \pm 0.0015\,\text{fm}, \\ a_s &= -23.7148 \pm 0.0043\,\text{fm}, \\ \rho_t(0,-\epsilon_t) &= 1.7436 \pm 0.0019\,\text{fm}, \\ \epsilon_s &= 66.26 \pm 0.05_{\text{stat}} + 0.14_{\text{syst}}\,\text{keV}. \end{aligned} \tag{9}$$

The errors are statistical, representing standard deviations. The one-sided systematic error shown for r_{s0} represents a one-standard-deviation error in its approximation to $\rho_s(0,0)$ and is obtained below. The one-sided systematic error on ϵ_s is propagated from the systematic error on r_{s0}, which is used instead of $\rho_s(0,-\epsilon_s)$ in Eq. (5), solved for γ_s, thus [47]

$$\gamma_s = r_{s0}^{-1}\left(1 - \sqrt{1 - 2r_{s0}/a_s}\right),$$

with $\epsilon_s = m_n + m_p - E$ following from Eq. (3), taking $p^2 = -\gamma_s^2$. An unknown contribution from Δr_s is neglected in ϵ_s. None of the other parameters have significant systematic errors.

A fit of r_t and r_s to the $T_{\max} = 3$ MeV data, holding a_t and a_s fixed at their values from Eq. (9), determines $\rho_t(0,0) = \lim_{T\to 0}\rho_t(0,T)$ and $\rho_s(0,0) = \lim_{T\to 0}\rho_s(0,T)$, but without a systematic contribution from Δr_t. Because r_t and r_s are correlated through $\partial r_s/\partial r_t \neq 0$, a two-step process is used to obtain statistically meaningful errors. First, $\rho_t(0,0)$ and $\rho_s(0,0)$ are fit. A new variable $\Delta\rho_t$ is then introduced as the sole fit parameter, with r_t and r_s constrained through

$$r_t = \rho_t(0,0) + \Delta\rho_t, \quad r_s = \rho_s(0,0) + \langle \partial r_s/\partial r_t\rangle \Delta\rho_t,$$

where $\langle \partial r_s/\partial r_t\rangle = 2.37465$ for the $T_{\max} = 3$ MeV data. The fit error of $\Delta\rho_t$ is determined as a standard deviation; $\Delta\rho_t$ fits to zero, $\chi^2_\nu = 0.747$, and

$$\begin{aligned} \rho_t(0,0) = 1.718 \pm 0.025\,\text{fm}, \quad \rho_s(0,0) = 2.696 \pm 0.059\,\text{fm}, \\ \Delta r_t = -0.025 \pm 0.025\,\text{fm}. \end{aligned} \tag{10}$$

The differences between $\rho_t(0,-\epsilon_t)$ and $\rho_t(0,0)$, and between r_{s0} and $\rho_s(0,0)$, are not significant, and Δr_t is not significantly different from zero. Because the downward shift in $\rho_s(0,0)$ relative to r_{s0} in Eq. (9) is very nearly the same as the statistical error on $\rho_s(0,0)$, this error is taken as the one-sided systematic error on r_{s0} anticipated in Eq. (6). The error on $\rho_t(0,0)$ in Eq. (10) has no bearing on $\rho_t(0,-\epsilon_t)$ in Eq. (9).

Figure 1 demonstrates the correlation between the fit values of $\rho_t(0,0)$ and $\rho_s(0,0)$. The shift in cross section above 1.5 MeV is almost negligible if both $\rho_t(0,0)$ and $\rho_s(0,0)$ are varied; there are too few and insufficiently precise data

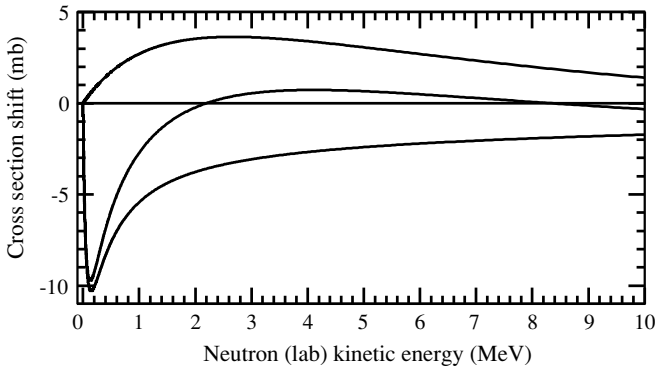

FIG. 1. The effect on the calculated cross section of the correlation between $\rho_t(0,0)$ and $\rho_s(0,0)$. (line at zero) $r_t = \rho_t(0,0)$, $r_s = \rho_s(0,0)$ from (10); (upper curve) $r_t = \rho_t(0,0) + 0.025$ fm, $r_s = \rho_s(0,0)$; (middle curve) $r_t = \rho_t(0,0) + 0.025$ fm, $r_s = \rho_s(0,0) + 0.059$ fm; and (lower curve) $r_t = \rho_t(0,0)$, $r_s = \rho_s(0,0) + 0.059$ fm.

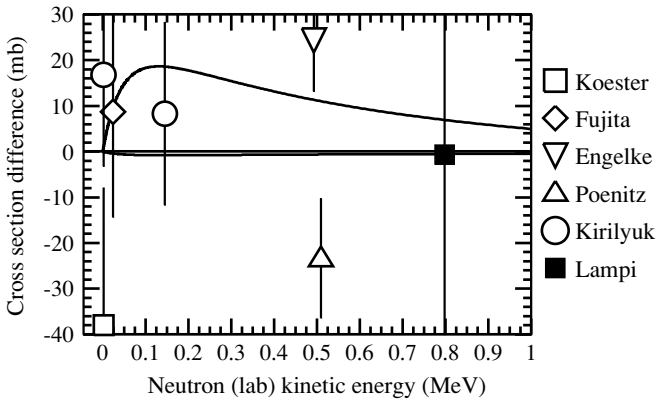

FIG. 2. Cross-section differences. The cross section calculated with the parameters from Eq. (9) is subtracted from data and calculations made with other choices of parameters. The curves form the one-standard-deviation envelope for the cross section calculated with $\rho_t(0,0)$ and $\rho_s(0,0)$ from Eq. (10); (line at zero) Shape-independent parameters from Eq. (9); (upper curve) $r_t = \rho_t(0,0) - 0.025$ fm, $r_s = \rho_s(0,0) - 0.059$ fm; and (lower curve) $r_t = \rho_t(0,0) + 0.025$ fm, $r_s = \rho_s(0,0) + 0.059$ fm. The lower curve is below and barely separated from the line. Data: [16] (Koester), [28] (Fujita), [17] (Engelke), [31] (Poenitz), [27] (Kirilyuk), and [32] (Lampi). Off-scale data are omitted; these have error bars that would span the entire vertical range of the plot.

below 1.5 MeV to break the correlation. Figure 2 emphasizes how poorly determined $\rho_t(0,0)$ and $\rho_s(0,0)$ are by the data available. Whether the reference line at zero or one of the curves describes the data better can hardly be decided. The peak in the upper curve occurs at 130 keV; a simultaneous determination of $\rho_t(0,0)$ and $\rho_s(0,0)$ is most sensitive to a measurement at this energy. The sensitivity falls to half-maximum at 23 and 620 keV; the useful data in this range are very sparse.

Improved low-energy cross-section measurements between about 20 and 600 keV are needed to overcome the correlation between $\rho_s(0,0)$ and $\rho_t(0,0)$. A single cross section with a precision of 0.4 mb near 130 keV would reduce the errors on $\rho_t(0,0)$ and Δr_t to about 0.001 fm. As it stands, Δr_t is more a measure of errors in the data than a measure of zero-energy shape dependence; it is insufficiently well determined to be of any use in a comparison with predictions from potential models.

ACKNOWLEDGMENTS

I am grateful to R. Chrien, S. U. Chung, and L. Trueman of BNL for their comments on the draft. This work was supported by the United States Department of Energy, under contract DE-AC02-98CH10886.

[1] H. P. Noyes, Phys. Rev. **130**, 2025 (1963).
[2] V. G. J. Stoks, R. A. M. Klomp, M. C. M. Rentmeester, and J. J. de Swart, Phys. Rev. C **48**, 792 (1993).
[3] V. Stoks and J. J. de Swart, Phys. Rev. C **52**, 1698 (1995).
[4] R. Machleidt and I. Slaus, J. Phys. G **27**, R69 (2001).
[5] R. B. Wiringa, V. G. J. Stoks, and R. Schiavilla, Phys. Rev. C **51**, 38 (1995).
[6] R. Machleidt, F. Sammarruca, and Y. Song, Phys. Rev. C **53**, R1483 (1996).
[7] S. Nakamura, T. Sato, V. Gudkov, and K. Kubodera, Phys. Rev. C **63**, 34617 (2001).
[8] R. Schiavilla, V. G. J. Stoks, W. Glöckle, H. Kamada, A. Nogga, J. Carlson, R. Machleidt, V. R. Pandharipande, R. B. Wiringa, A. Kievsky *et al*., Phys. Rev. C **58**, 1263 (1998).
[9] G. Q. Li and R. Machleidt, Phys. Rev. C **58**, 3153 (1998).
[10] G. A. Miller, M. K. Nefkens, and I. Šlaus, Phys. Rep. **194**, 1 (1990).
[11] S. Klarsfeld, J. Martorell, and D. W. L. Sprung, J. Phys. G **10**, 165 (1984).
[12] R. Machleidt, Phys. Rev. C **63**, 24001 (2001).
[13] E. Melkonian, Phys. Rev. **76**, 1744 (1949).
[14] T. L. Houk, Phys. Rev. C **3**, 1886 (1971).
[15] W. Dilg, Phys. Rev. C **11**, 103 (1975).
[16] L. Koester, W. Waschkowski, and J. Meier, Z. Phys. A **337**, 341 (1990).
[17] C. E. Engelke, R. E. Benenson, E. Melkonian, and J. M. Lebowitz, Phys. Rev. **129**, 324 (1963); data from CINDA, file EXFOR 11118.002 and 11118.003.
[18] R. Wilson, *The Nucleon-Nucleon Interaction, Experimental and Phenomenological Aspects* (Interscience, New York, 1963).
[19] Equation (2) is not usually written as a single equation, except in Ref. [18]. Usually, one finds $\sigma_d = 4\pi p^{-2} \sin^2 \delta_d$, with $p \cot \delta_d = -a_d^{-1} + \frac{1}{2}\rho_d(0,T)p^2$, both of which are exact.
[20] H. A. Bethe, Phys. Rev. **76**, 38 (1949).
[21] Occasionally in the literature there is something like $a_c = (3a_t + a_s)/4\mu$, e.g., Ref. [2], where μ is the H_2 molecular mass correction, $\mu \approx \frac{1}{2}$. This is not correct. a_c is *defined* by Eq. (8), or $a_c \equiv 2(\frac{3}{4}a_t + \frac{1}{4}a_s)$, where the factor 2 arises because there are two indistinguishable protons. The molecular mass correction correctly occurs in the relation between the coherent cross section and a_c. See Refs. [18,48].
[22] L. Koester and W. Nistler, Phys. Rev. Lett. **27**, 956 (1971).
[23] J. Callerame, D. J. Larson, S. J. Lipson, and R. Wilson, Phys. Rev. C **12**, 1423 (1975).
[24] L. Koester and W. Nistler, Z. Phys. A **272**, 189 (1975).
[25] V. F. Sears, Z. Phys. A **321**, 443 (1985).
[26] Nuclear Data Centers Network, *CINDA, Index to the Literature and Computer Files on Microscopic Neutron Data* (International Atomic Energy Agency, Vienna, Austria, 2004). Information extracted from the CINDA database, version 2004, http://www.nndc.bnl.gov/index.jsp, as of 1 September 2004.
[27] A. L. Kirilyuk, A. V. Grebnev, P. N. Vorona, and N. L. Gnidak, **C87KIEV2**, 298 (1987); data from CINDA, file EXFOR 40980.004.
[28] Y. Fujita, K. Kobayashi, T. Oosaki, and R. C. Block, Nucl. Phys. **A258**, 1 (1976).
[29] W. D. Allen and A. T. G. Ferguson, Proc. Phys. Soc. A **68**, 1077 (1955); data from CINDA, file EXFOR 21364.002 and 21364.003.

[30] C. D. Bailey, W. E. Bennett, T. Bergstralth, R. G. Nuckolls, H. T. Richards, and J. H. Williams, Phys. Rev. **70**, 583 (1946); data from CINDA, file EXFOR 11140.002.
[31] W. P. Poenitz and J. F. Whalen, Nucl. Phys. **A383**, 224 (1982); data from CINDA, file EXFOR 12715.002.
[32] E. E. Lampi, G. D. Freier, and J. H. Williams, Phys. Rev. **80**, 853 (1950); data from CINDA, file EXFOR 12644.003.
[33] R. E. Fields, R. L. Becker, and R. K. Adair, Phys. Rev. **94**, 389 (1954); data from CINDA, file EXFOR 11073.002.
[34] L. Koester, W. Waschkowski, J. Meier, G. Rau, and M. Salehi, Z. Phys. A **330**, 387 (1988); data from CINDA, file EXFOR 22105.002.
[35] C. L. Storrs and D. H. Frisch, Phys. Rev. **95**, 1252 (1954).
[36] R. B. Schwartz, R. A. Schrack, and H. T. Heaton, Phys. Lett. **B30**, 36 (1969); data from CINDA, file EXFOR 10005.003.
[37] J. C. Davis and H. H. Barschall, Phys. Rev. C **3**, 1798 (1971); data from CINDA, file EXFOR 10099.003.
[38] J. M. Clement, P. Stoler, C. A. Goulding, and R. W. Fairchild, Nucl. Phys. **A183**, 51 (1972); data from CINDA, file EXFOR 10173.003.
[39] N. Nereson and S. Darden, Phys. Rev. **89**, 775 (1953); data from CINDA, file EXFOR 11060.002.
[40] E. M. Hafner, W. F. Hornyak, C. E. Falk, G. Snow, and T. Coor, Phys. Rev. **89**, 204 (1952).
[41] D. C. Larson, J. A. Harvey, and N. W. Hill, ORNL **5787**, 174 (1980); data from CINDA, file EXFOR 12882.002.
[42] D. G. Foster, Jr. and D. W. Glasgow, Phys. Rev. C **3**, 576 (1971); data from CINDA, file EXFOR 10047.002.
[43] C. F. Cook and T. W. Bonner, Phys. Rev. **94**, 651 (1954); data from CINDA, file EXFOR 11074.002.
[44] J. C. Davis and H. H. Barschall, Phys. Lett. **B27**, 636 (1968).
[45] E. G. Kessler Jr., M. S. Dewey, R. D. Deslattes, A. Henins, H. G. Börner, M. Jentschel, C. Doll, and H. Lehmann, Phys. Lett. **A255**, 221 (1999).
[46] Particle Data Group, Phys. Lett. **B592**, 1 (2004).
[47] L. P. Kok, Phys. Rev. Lett. **45**, 427 (1980).
[48] J. M. Blatt and V. F. Weisskopf, *Theoretical Nuclear Physics* (Wiley, New York, 1952).